Noname manuscript No.
(will be inserted by the editor)

Mesh local refinement to enhance effusion cooling models

R. Bizzari[a] * · M. Férand[a] · A. Dauptain[a] · G. Staffelbach[a] · S. Richard[b] · J.-D. Muller[c] · T. Ogier[b] · G. Exilard[b] · F. Nicoud[d]

Abstract In aeronautical combustors, effusion cooling is the preferred technique used to shield walls from the hot gases. Jets from thousands of sub-millimeter angled perforations form a film isolating the liner. When performing a Large Eddy Simulation (LES) of a real engine, including effects of the effusion cooling is a challenge. A modeling technique [1] has been developed recently to address this issue. However in that work, the precision is still relative to the mesh. The present study proposes an automatic adaptive method which increases the mesh resolution in key areas allowing to achieve more accurate results at moderate additional cost.

Keywords Combustor · LES · Effusion cooling · Modeling · Adaptive Mesh Refinement

1 Introduction

In aeronautical combustion chambers, the temperature of the burnt gases exceeds the thermal wall resistance, thus requiring methods to cool the liner [2]. Effusion cooling [3] is widely used since it is both efficient and lightweight. Multi-perforated liners operate on the same principle as a porous walls except that the cooling flow is injected through discrete, laser-drilled sub-millimeter holes [4]. A industrial combustor would have thousands of effusion holes, however a Large Eddy Simulations (LES) where all holes are resolved will not be feasible before 2050 [5]. As an alternative, models for effusion cooling have been developed [6–11]. The homogeneous model by Mendez et al. [7] is a first approximation where the multi-perforated liner is represented as a homogeneous boundary condition which injects the appropriate mass flow and momentum [12]. Although numerically convenient, this approach excludes any local effects due to the discrete nature of the holes. The limitation to homogeneous models means that the LES relies on a fully modeled representation of the effusion plates, similar to that of RANS, although the computational resources available today only allow mesh resolution approaching the aperture diameter. Therefore, a more precise model is essential in order to take advantage of LES when dealing with combustors with effusion cooling. The so-called thickened-hole model was recently proposed in this framework [1]. In this model, the apertures of the perforated liner are thickened in order to impose a minimum of 3 cells in the numerical diameter of the jet regardless of the mesh size. Modeling ideas developed for the homogeneous model [7,12] are then adapted in order to maintain the correct mass and momentum fluxes [1]. The thickened-hole model thus shares the properties of the homogeneous model when the grid is coarse. However, if the mesh cell size Δx is sufficiently fine at the wall, local effects near the actual hole can be captured. The ratio R defined in [1] quantifies the mesh resolution with respect to the diameter d of the holes : $R = d/\Delta x$. The heterogeneous model begins to show locally non-stationary phenomena with R values greater than unity ($R = 4$, say) but much smaller than the resolution needed for an LES to correctly resolve a jet-in-crossflow situation (R=20-30, say). However, the actual practice in gas turbine manufacturers, such as Safran Helicopter Engines, is to perform LES of combustors with grids corresponding to R close to unity, making the result of the thickened-hole model [1] equivalent to, but not significantly better than homogeneous model. To increase the ratio R, a finer mesh is needed, but out of reach *a priori*: going to a mesh at $R = 4$ would increase the cost of an explicit simulation by at least a factor of 32.

The purpose of this paper is to study an alternative solution using adaptive mesh refinement in order to achieve better results at an affordable cost. The test case is first described, then two 'Mesh Local Refinement' methods MLR1 and MLR2 are presented with particular attention to the mesh and properties resulting from each method. Finally, both methods are applied to an industrial case.

[a] CERFACS - 42, Av. Gaspard Coriolis, 31057 Toulouse cedex 1, France
[b] Safran Helicopter Engine - 25, Av. Joseph Szydlowski, 64510 Bordes, France
[c] SEMS, Queen Mary University of London, Mile End Road, United Kingdom
[d] IMAG, Univ Montpellier, CNRS, Montpellier, France
* E-mail: romain.bizzari@cerfacs.fr

2 Academical test case

The academical test case used is the Maveric-H test case which has already been studied in several papers [13–16]. It consists of two parallel channels communicating through 144 holes. Thanks to the periodicity of the setup, only 12 holes can be computed. The hole diameter (d) equals 0.4 mm. Blowing ($M = \rho_{jet}V_{jet}/\rho_{hot}U_{hot}$) and momentum ($J = \rho_{jet}V_{jet}^2/\rho_{hot}U_{hot}^2$) ratios are 8.4 and 31 respectively. A holes resolved simulation where both sides of the multi-perforated plate are computed is considered as the reference. Extracting the mass flux from this simulation allows computing only the injection side in the simulations with effusion cooling model. In [1], it has been shown that the result is highly dependent on the R ratio. With $R = 2$ the jets from the aperture do not penetrate enough whereas with $R = 4$ the results are very close to those obtained by the resolved simulation. In addition, jets and inter rows profiles are distinct with $R = 4$ which is not the case when $R = 2$. Going from $R = 2$ to $R = 4$ leads to a huge improvement on the result in return to a much higher cost. A local mesh adaptation where only the key areas are refined would reduce the cost. In this study, two uniform meshes corresponding to $R = 2$ and $R = 4$ and two adapted meshes MLR1 and MLR2 (named by the adaptive method used to obtain the corresponding mesh) are used as shown in Fig. 1.

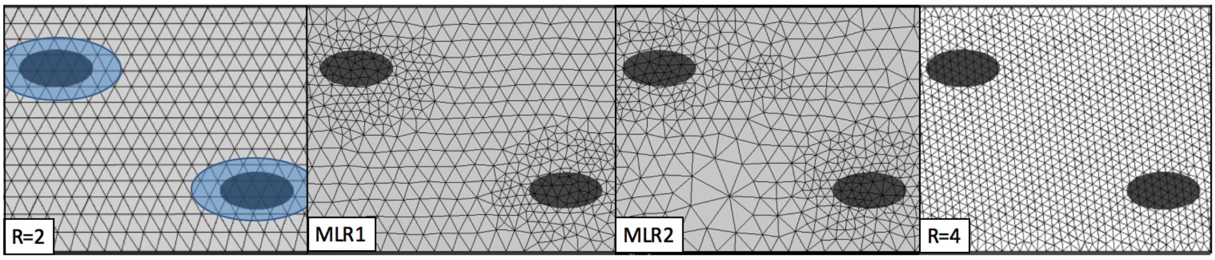

Fig. 1: Superposition of real size multiperforation holes (black ellipse) on the wall for different grids ratio: $R = 2$; $R = 2$ with MLR1 adaptation; $R = 2$ with MLR2 adaptation; $R = 4$. The enlarged holes are also highlighted on the $R = 2$ case (light blue ellipse). No enlargement was used for the other cases since the mesh corresponds for R=4 in these cases.

Hip (www.cerfacs.fr/avbp7x/hip.php) and MMG3D [17] libraries were used to adapt the mesh and generate MLR1 and MLR2 from the uniform one at R=2. For the MLR1 case, starting from a uniform $R = 2$ mesh, a geometrical strategy of refinement name MLR1 has been used. Only the cells at a distance lower than 3 diameters of the hole were refined leading to $R = 4$ in this area. With this method, no thickening is needed. As the modeled area is reduced with MLR1, a second adaptation (MLR2), based on physical quantities from MLR1's solution can be proposed. Note that it only need a short physical time to be computed since the instantaneous field close to the effusion jets is sufficient. The aim of this MLR2 adaptation is to reduce the cost without losing physical information. Starting from a uniform mesh at $R = 2$, high velocity and low temperature zones were refined while the others were coarsened. This strategy leads to a drastic reduction of the total number of nodes and thus reduces the over-cost. The main properties of the cases are presented in Table 1 were CPU_{adim} time is the cost to simulate a typical physical time of the configuration, taking the $R = 2$ case as the reference. σ_n stands for the ratio between the real geometrical hole surface and its numerical counterpart.

Case	R at the aperture	Cells	σ_n	CPU_{adim}
$R = 2$	2	858 459	0.48	1
MLR1	4	874 652	1	2.4
MLR2	4	405 343	1	1.2
$R = 4$	4	6 705 379	1	14.9
Resolved	16	51 077 506	1	510

Table 1: Characteristics of the meshes.

The results on the Maveric-H test case are presented in Fig 2. The $R = 2$ field of temperature shows no fluctuation and mostly looks like a laminar flow. On the contrary, for the $R = 4$ case, temperature variations are visible and small structures appear. When using either MLR1 or MLR2, results are quite similar and in both cases jets and inter jets areas can be distinguished. Wall temperature is also better predicted than for the R=2 case. In Fig. 3, temperature and axial mass flow-rate profiles are presented. 3D data is temporally and spatially averaged in the spanwise direction and presented as a function of Y^*, the distance from the plate normalized by

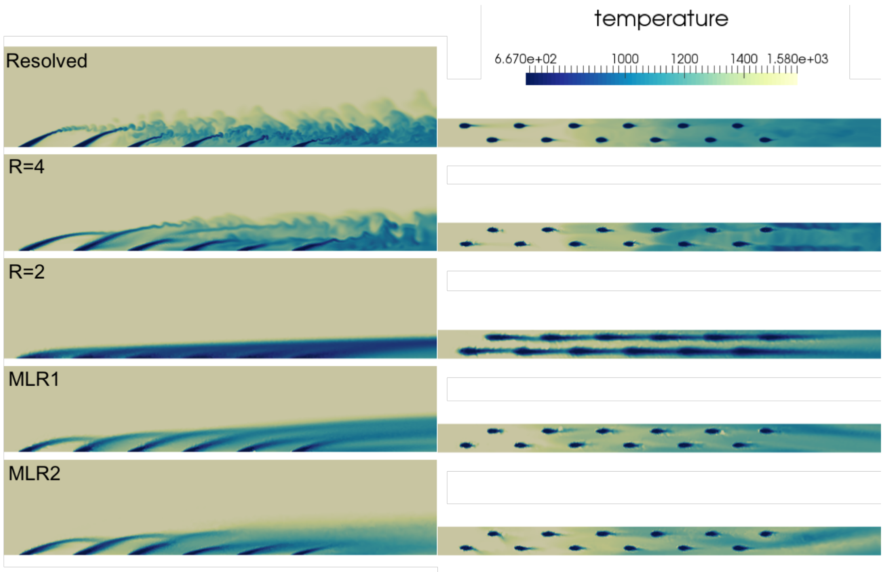

Fig. 2: Instantaneous temperature fields through one row of holes (left) and on the wall (right) for each case.

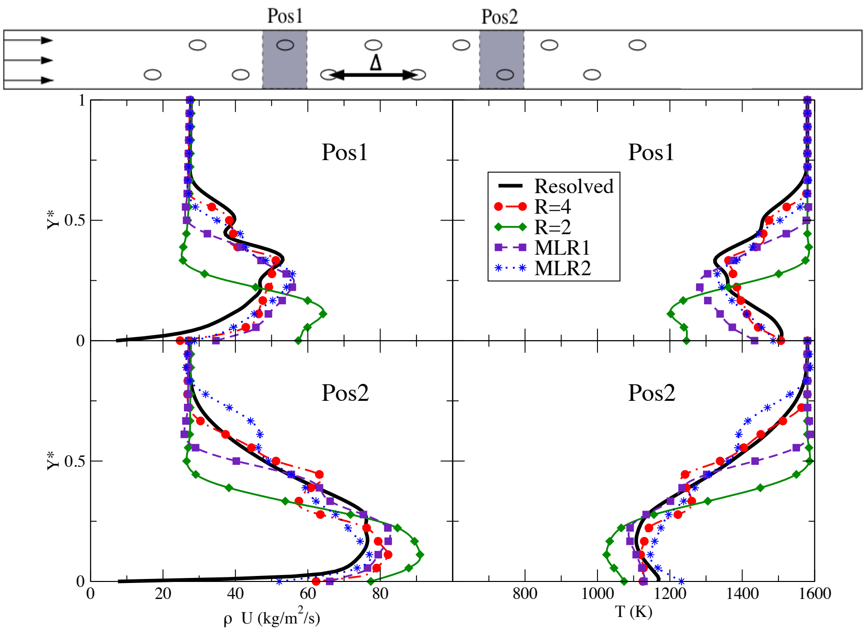

Fig. 3: Temperature (right) and streamwise mass flow-rate (left) profiles are presented for 2 plate positions: Pos1 (upper part) and Pos2 (lower part).

the inter-row distance Δ defined in Fig. 3 ($\Delta = 11.68d$). Results are presented for 2 positions. The $R = 2$ case does not recover the same shape as the reference solution and the jets penetrate 40% less than for the resolved case. In adapted cases results are closer (24% less for MLR1 and 8% more penetration for MLR2). In short, MLR2 provides results similar to $R = 4$ for less than one tenth the price of the computation. It also outperforms $R = 2$ for only 20% CPU cost increase.

3 Application on a real combustor

These MLR methods have been applied to one sector of a turboshaft reverse flow combustion chamber (see Fig 4) already studied and presented in [18,16]. Since the initial mesh (M_0) has a very low R resolution a first MLR1 adaptation has been performed which lead to M_1. Note also that cells located on the wall and between jets are coarsened. A second MLR1 without coarsening between jets has been performed in order to obtain M_2. Thanks to the results from M_2, a M_{2bis} mesh has been obtained using the so-called MLR2 method. A M_3 has been created from the M_2 mesh using MLR1 method in order to have a relative convergence comparison (with

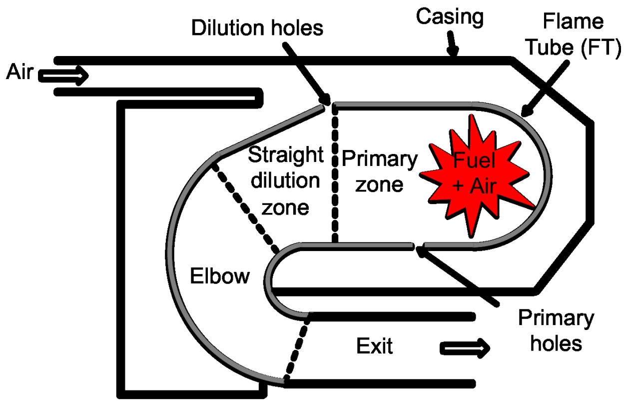

Fig. 4: Schematic view of the combustor extracted from Berger *et al.* [18].

a distance of influence of 6 hole diameters instead of 3). Properties of different meshes are provided in Table 2. CPU_{adim} corresponds to the CPU cost normalized by the CPU cost of the M_0 case (40 000 h CPU for 30ms physical time).

Case	Refinement method	R at the aperture	Cells	σ_n	CPU_{adim}
M_0	N/A	0.75	45 892 340	0.06	1
M_1	MLR1 from M_0	2.25	54 417 508	0.56	2.8
M_2	MLR1 from M_1	4.5	115 523 143	1	14.6
M_{2bis}	MLR2 from M_1	4.5	72 484 864	1	4.0
M_3	MLR1 from M_2	6	242 437 477	1	31.1

Table 2: Characteristics of the meshes for the real combustor.

On Fig. 5(a), a zoom on the boundary of the combustor shows the evolution of the injected surface (dark grey) in function of the grid resolution. Thickening due to the modeling are visible on M_0 and M_1 while it is not the case for other cases. Note that the R ratio corresponds to the number of cells into the aperture's diameter (smaller diameter of the minor axis of the ellipse), however since the grid is non uniform more cells can be counted.

On Fig. 5(b), the inner mesh is visible, the temperature field from the instantaneous corresponding simulation is displayed. The aerodynamic field is very different; similar conclusion as on the Maveric test case can be drawn: on the M_0 case, the cold layer is uniform while in the M_3 case a jet is visible. M_2 and M_{2bis} give very close results and allow to capture the jet induced by the effusion holes while in terms of CPU cost the M_{2bis} case is less expensive. In this case, only key zones of the jet are refined.

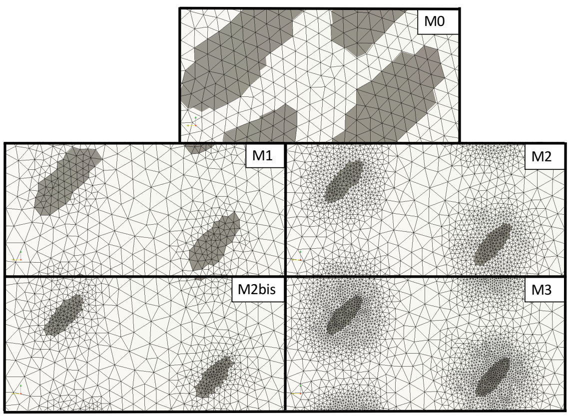

(a) Boundary with the projection of the multiperforated holes with the thickened-hole model.

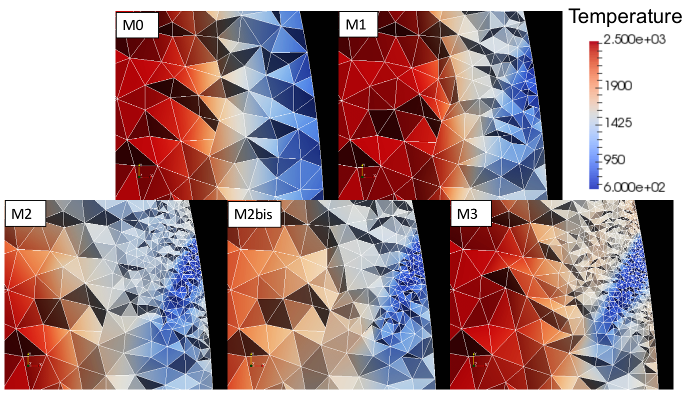

(b) Cut through a hole. Visualization of the jet resulting from the corresponding instantaneous simulations.

Fig. 5: Local effects of the mesh on a real combustor.

Temperature of the liner is compared to experimental measurements in Fig. 7. However a large computational time is required to assess time averaged solution and thus only the M0 and the M1 cases are available so far (see Table 2). The provided experimental data comes from thermocolor tests as described in [18,16]. This explains the broad range of experimental data at a given location. Thermocolor indeed give only access to a temperature range, but has the advantage of allowing to characterize the whole combustor temperature field. Since the computation is adiabatic, the simulations are averaged in time to obtain mean velocity and temperature fields and are then post processed using correlations from Cottin [19] and estimator from Bizzari *et al.* [16]. Figure 7 shows a comparison between numerical and experimental data as a function of the axial position (x) for two lines defined in Fig. 6. Both numerical simulations are very close to the experimental results. However the M1 simulation gives closer results. It highlights the fact that the thickened-hole model combined with an adaptive mesh refinement methods increases the efficiency of the wall temperature prediction for aeronautical combustors. In particular, the hot zone close to the combustor dome (low flame tube abscissa, noted Do on Fig. 6) is better captured by mesh M_1. In the same way, temperature levels in the range of abscissa [0.04-0.08] is in better agreement with experiments for this mesh. In addition, the temperature level is higher and better predicted with adapted mesh than with the standard mesh (M_0), demonstrating that a less coherent cooling film is directly resolved, as shown on the academic case.

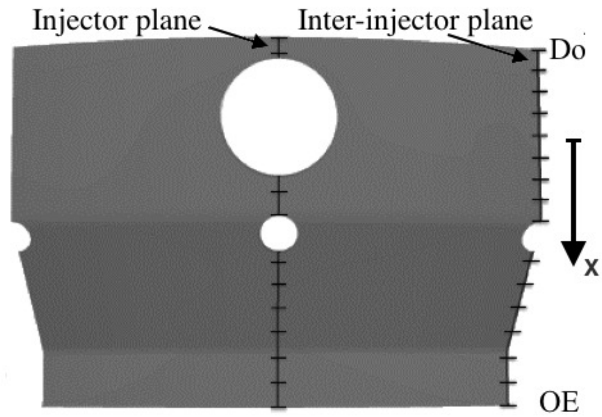

Fig. 6: Definition of the injector plane and inter-injector plane lines.

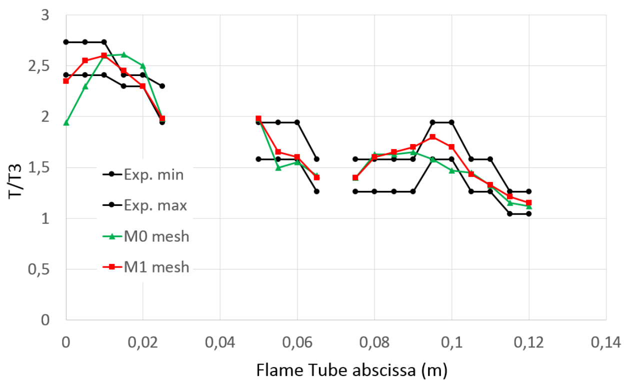

(a) Injector plane.

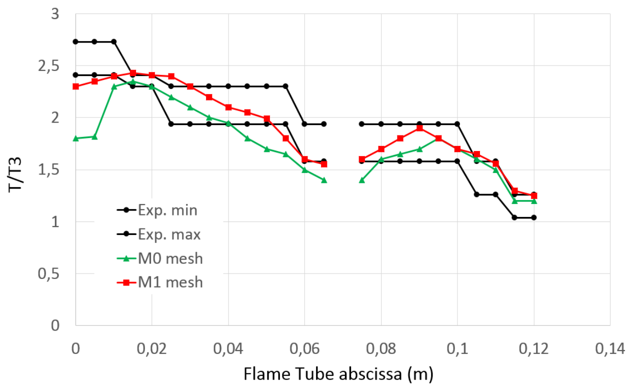

(b) inter injector plane

Fig. 7: Comparison between experimental thermocolor measurements and results from M_0 and M_1.

4 Conclusion

The present study shows how mesh adaption combined with a heterogeneous model of effusion cooling can yield significant improvement in accuracy of industrial Large Eddy Simulations for the design process of modern combustors. To our knowledge this is the first attempt of mesh adaption focused specifically on modeling effusion cooling. Heterogeneous modeling is a recent technique which can benefit from a higher mesh resolution, but the computational power currently available does not allow to achieve a significant breakthrough with standard meshing techniques. Indeed, the benefits given by the heterogeneity of the thickened-hole model need a wall ratio R larger than 4 which it is still lower than what is feasible in uniformly refined meshes. With a brute force global refinement, such resolution will not be achieved before another 10 years. Mesh adaption allows to reach local wall ratios of $R = 4$ which is feasible with present computational power. The present study shows on an academic test case how to define a refinement metric satisfying both a resolution requirement near the jets and a satisfactory mesh coarsening between holes. As a result, adapted meshes exhibit features similar to brute force meshes, yet for a much more affordable CPU cost. The same approach was also tested on a complex case with thousands of holes, with results significantly improved for both local effects and global trends.

Acknowledgements This work was granted access to the HPC resources of CEA and CERFACS.

References

1. R. Bizzari, D. Lahbib, A. Dauptain, F. Duchaine, L.Y.M. Gicquel, and F. Nicoud. A thickened-hole model for large eddy simulations over multiperforated liners. Flow Turbulence and Combustion, Online First Articles:1–13, 2018.
2. Richard J Goldstein. Film cooling. Advances in heat transfer, 7:321–379, 1971.
3. A. H. Lefebvre. Gas Turbines Combustion. Taylor & Francis, 1999.
4. R. Poprawe, I. Kelbassa, K. Walther, M. Witty, D. Bohn, and R. Krewinkel. Optimising and manufacturing a laser-drilled cooling hole geometry for effusion-cooled multi-layer plates. Proc. of ISROMAC-12, Paper, (20091), 2008.
5. D Lahbib. Modélisation aérodynamique et thermique des multiperforations en les. PhD, Université Montpellier II, 2015.
6. André Burdet, Reza S Abhari, and Martin G Rose. Modeling of Film Cooling—Part II: Model for Use in Three-Dimensional Computational Fluid Dynamics. Journal of turbomachinery, 129(2):221–231, 2007.
7. S. Mendez and F. Nicoud. Adiabatic homogeneous model for flow around a multiperforated plate. AIAA Journal , 2008.
8. Stefan Voigt, Berthold Noll, and Manfred Aigner. Development of a macroscopic CFD model for effusion cooling applications. ASME Paper No. GT2012-68251, 2012.
9. Samir Rida, Robert Reynolds, S Chakracorty, and Kapil Gupta. Imprinted effusion modeling and dynamic cd calculation in gas turbine combustors. ASME Paper No. GT2012-68804, 2012.
10. L. Mazzei, A. Andreini, and B. Facchini. Assessment of modelling strategies for film cooling. International Journal of Numerical Methods for Heat & Fluid Flow, 27(5):1118–1127, 2017.
11. Alejandro M Briones, Brent A Rankin, Scott D Stouffer, Timothy J Erdmann, and David L Burrus. Parallelized, automated, and predictive imprint cooling model for combustion systems. Journal of Engineering for Gas Turbines and Power, 139(3):031505, 2017.
12. S. Mendez and F. Nicoud. Large-eddy simulation of a bi-periodic turbulent flow with effusion. J. Fluid Mech. , 2008.
13. J.-L. Florenciano and P. Bruel. LES fluid–solid coupled calculations for the assessment of heat transfer coefficient correlations over multi-perforated walls. Aerospace Science and Technology, 53:61 – 73, 2016.
14. P. Miron. Étude expérimentale des lois de parois et du film de refroidissement produit par une zone multiperforée sur une paroi plane. Phd thesis, Université de Pau et des Pays de l'Adour, 2005.
15. B. Petre, E. Dorignac, and J. J. Vullierme. Study of the influence of the number of holes rows on the convective heat transfer in the case of full coverage film cooling. Int. J. Heat and Mass Transfer , 2003.
16. R. Bizzari, D. Lahbib, A. Dauptain, F. Duchaine, S. Richard, and F. Nicoud. Low order modelling method for assessing the temperature of the multi-perforated plates. Submitted to Int. J. Heat and Mass Transfer , 2018.
17. Cécile Dobrzynski and Pascal Frey. Anisotropic delaunay mesh adaptation for unsteady simulations. In Proceedings of the 17th international Meshing Roundtable, pages 177–194. Springer, 2008.
18. S. Berger, S. Richard, Staffelbach G., F. Duchaine, and L. Gicquel. Aerothermal prediction of an aeronautical combustion chamber based on the coupling of large eddy simulation, solid conduction and radiation solvers. GT2015-42457, June 2015.
19. G. Cottin, E. Laroche, N. Savary, and P. Millan. Modeling of the heat flux for multi-hole cooling applications. In ASME 2011 Turbo Expo: Turbine Technical Conference and Exposition, pages 1955–1965. American Society of Mechanical Engineers, 2011.